**Atmospheric
Measurement
Techniques
Discussions**

# Site selective real-time measurements of atmospheric $N_2O$ isotopomers by laser spectroscopy

J. Mohn[1], B. Tuzson[1], A. Manninen[1], N. Yoshida[2], S. Toyoda[2], W. A. Brand[3], and L. Emmenegger[1]

[1]Laboratory for Air Pollution & Environmental Technology, Empa, Dübendorf, Switzerland
[2]Department of Environmental Chemistry and Engineering, Tokyo Institute of Technology, Yokohama, Japan
[3]Max-Planck-Institute for Biogeochemistry, Jena, Germany

Title Page

Abstract | Introduction

Conclusions | References

Tables | Figures

|◄ | ►|

◄ | ►

Back | Close

Full Screen / Esc

Printer-friendly Version

Interactive Discussion

## Abstract

We describe the first high precision real-time analysis of the N$_2$O site-specific isotopic composition at ambient mixing ratios. Our technique is based on mid-infrared quantum cascade laser absorption spectroscopy (QCLAS) combined with an automated preconcentration unit. The QCLAS allows for simultaneous and specific analysis of the three main stable N$_2$O isotopic species, $^{14}$N$^{15}$N$^{16}$O, $^{15}$N$^{14}$N$^{16}$O, $^{14}$N$^{14}$N$^{16}$O, and the respective site-specific relative isotope ratio differences $\delta^{15}$N$^\alpha$ and $\delta^{15}$N$^\beta$. Continuous, stand-alone operation is achieved by using liquid nitrogen free N$_2$O preconcentration, a quasi-room-temperature quantum cascade laser (QCL), quantitative sample transfer to the QCLAS, and an optimized calibration algorithm. The N$_2$O site-specific isotopic composition ($\delta^{15}$N$^\alpha$ and $\delta^{15}$N$^\beta$) can be analysed with a long term precision of 0.2‰. The potential of this analytical tool is illustrated by continuous N$_2$O isotopomer measurements above a grassland plot over three weeks period, which allowed identification of microbial source and sink processes.

## 1 Introduction

Nitrous oxide (N$_2$O) is the most important anthropogenically emitted ozone depleting substance and also a significant greenhouse gas (Ravishankara et al., 2009). N$_2$O mixing ratios in the troposphere increased from 270 ppb to the current level of 321.6 ppb (AGAGE 2008) at 0.8 ppb yr$^{-1}$ (2005 to 2008) with more than one third of N$_2$O emissions being anthropogenic (Montzka et al., 2011; Solomon et al., 2007). For a better understanding of source and sink processes, however, the information obtained from measuring the intramolecular distribution of $^{15}$N on the central ($\alpha$) and the end ($\beta$) position of the linear N$_2$O molecule is crucial (Yoshida and Toyoda, 2000).

Abundances of the different isotopic species ($^{14}$N$^{14}$N$^{16}$O, $^{14}$N$^{15}$N$^{16}$O, $^{15}$N$^{14}$N$^{16}$O, etc.) are usually reported in the $\delta$-notation, where $\delta^{15}$N denotes the relative difference in the amount of $^{15}$N versus $^{14}$N (abbreviated herein as $^{15}$N/$^{14}$N) in N$_2$O in comparison

to atmospheric $N_2$ as the reference material (Coplen, 2011). Similarly, $\delta^{15}N^\beta$ denotes the relative difference of isotope ratios for $^{15}N^{14}N^{16}O$ vs. $^{14}N^{14}N^{16}O$.

The bulk nitrogen $\delta$ value ($\delta^{15}N^{bulk} = (\delta^{15}N^\alpha + \delta^{15}N^\beta)/2$) of tropospheric $N_2O$ is enriched by $6.3 \pm 0.3$‰ to $6.72 \pm 0.12$‰, depending on the sampling location and time (Kaiser et al., 2003; Park et al., 2004; Röckmann and Levin, 2005; Toyoda et al., 2004), with a strong site preference (SP = $\delta^{15}N^\alpha - \delta^{15}N^\beta$) of $18.7 \pm 2.2$‰ for the central nitrogen atom (Yoshida and Toyoda, 2000). Temporal trends in the $N_2O$ isotopic composition from firn air, ice core and archived air sample measurements indicate a year to year decrease in $\delta^{15}N^{bulk}$ of $0.04$‰ $yr^{-1}$, confirming substantial emissions of isotopically depleted $N_2O$ (Bernard et al., 2006; Ishijima et al., 2007; Röckmann and Levin, 2005). According to isotopic budgetary calculations based on a simple two-box model, this could be due to increased anthropogenic $N_2O$ emission from agricultural soils, as well as a to a change in their average isotopic signature (Ishijima et al., 2007).

On a local scale, the $N_2O$ isotopic composition can be applied to disentangle or even quantitatively apportion $N_2O$ production and destruction pathways. For example, the $^{15}N$ depletion in $N_2O$ produced by autotrophic nitrification was found to be considerably higher as compared to heterotrophic denitrification (Koba et al., 2009; Sutka et al., 2006; Toyoda et al., 2005; Yoshida, 1988). On the other hand, process-specific effects on $\delta^{15}N^{bulk}$ might be masked by shifts in the precursor signature (Well et al., 2008), and theoretical considerations indicate a major impact of the involved bacterial species (Schmidt et al., 2004). In contrast to $\delta^{15}N^{bulk}$, the site preference is considered to be independent of the isotopic composition of the precursor and thus supplies clear process information even if the isotopic signature of the substrate for $N_2O$ production is lacking (Frame and Casciotti, 2010; Ostrom et al., 2007; Sutka et al., 2006; Toyoda et al., 2002; Well and Flessa, 2009; Yamagishi et al., 2007).

The standard technique for $N_2O$ isotopic measurements is laboratory-based isotope-ratio mass-spectrometry (IRMS) in combination with flask-sampling (Brenninkmeijer and Röckmann, 1999; Toyoda and Yoshida, 1999). It is a well-known method with excellent precision of up to $0.05$‰ for $\delta^{15}N^{bulk}$, $0.1$‰ for $\delta^{18}O$, and $0.3$‰ for $\delta^{15}N^\alpha$

and $\delta^{15}N^{\beta}$ (Bernard et al., 2006; Toyoda et al., 2011a,b). Nevertheless, it also has some disadvantages such as the large size of the instrument, which hinders in-situ field measurements. Laser spectroscopy is a valuable alternative because it is inherently selective, even for molecules with the same mass (Janssen and Tuzson, 2006; Gagliardi et al., 2005; Nakayama et al., 2007; Uehara et al., 2001, 2003; Wächter and Sigrist, 2007), and field-deployable instruments for unattended measurements can be designed. A significant improvement was obtained in recent years by the implementation of quantum cascade laser sources (QCL) to reach a precision of 0.5‰ for $\delta^{15}N^{\alpha}$ and $\delta^{15}N^{\beta}$ at $N_2O$ mixing ratios of 90 ppm (Wächter et al., 2008).

In the present project we describe the first instrumentation to perform real-time analysis of $N_2O$ site-specific isotopic composition at atmospheric mixing ratios. This is achieved combining a liquid nitrogen-free fully-automated preconcentration unit optimized and validated for $N_2O$ isotopomer analysis by Mohn et al. (2010) with an improved version of the QCLAS published by Wächter et al. (2008). The potential of this approach is demonstrated by a three week measurement campaign of atmospheric $N_2O$ to identify distinct soil microbial $N_2O$ source and sink processes.

## 2  Materials and methods

A schematic diagram of the measurement setup is shown in Fig. 1. Details on the development, optimization and validation of the $N_2O$ preconcentration unit and the QC laser spectrometer have been described previously (Mohn et al., 2010; Wächter et al., 2008). Thus, their basic principles and recent modifications are only briefly presented, while analytical improvements, procedures of air sampling, automation and the applied calibration procedure are discussed in more detail.

## 2.1 Sampling site and setup

Field experiments were conducted in Dübendorf at 430 m a.s.l. (47°24′10″ N/8°36′43″ E). The observation area is located in an industrial and densely populated region near Zurich. A main road passes 100 m south, and a high-
5　way around 750 m north of the sampling site. Air was continuously sampled above a grassland plot (5 m × 20 m) at a flow rate of about one standard litre per minute (slpm) through a 15 m long unheated PTFE tubing (ID 4 mm) using a diaphragm vacuum pump (KNF Neuberger, CH). The air intake was first mounted at 1.5 m above ground (8 to 24 September), and then (24 to 31 September) 10 cm above the surface to be more
10　representative for soil $N_2O$ production. At the pump outlet, the pressure was adjusted to 4 bar by means of a pressure relief valve. Water and $CO_2$ were quantitatively removed by permeation drying (PD-100T-48, PermaPure Inc., USA) and by chemical trapping with Ascarite (30 g, 10–35 mesh, Fluka, Switzerland) bracketed by $Mg(ClO_4)_2$ (2 × 13 g, Fluka, Switzerland). Finally, the sample was passed through a sintered metal
15　filter (SS-6F-MM-2, Swagelok, USA) and directed to the preconcentration unit. An alternative sample input consisted of pressurized air (Messer, Switzerland) employed as target gas (Klausen et al. 2010) which was treated as described above by a second permeation dryer and a chemical trap (20 g Ascarite, 2 × 8 g $Mg(ClO_4)_2$). This setup allows determining the long term stability and precision of the complete analytical
20　procedure, including preconcentration, laser spectroscopic analysis and calibration. The chemical traps were exchanged every 3 to 4 days before reaching their maximal load. To detect any potential breakthrough, the $CO_2$ concentration was monitored by QCLAS after preconcentration together with the $N_2O$ isotopomers ($CO_2$ line at 2188.0 cm$^{-1}$).

## 2.2 Instrumentation

### 2.2.1 N$_2$O preconcentration

The technology of our preconcentration unit is based on a previously developed system called "Medusa" (Miller et al., 2008), re-designed and optimized for the preconcentra-
tion of N$_2$O isotopic species and their subsequent quantification by laser spectroscopy (Mohn et al., 2010). During standard operation, 10 l of ambient air are preconcentrated on a HayeSep D trap and desorbed in approximately 50 ml of synthetic air, yielding a concentration increase from ambient mixing ratios to >71 ppm N$_2$O. The system of-
fers quantitative (>99 %) N$_2$O recovery without any significant isotopic fractionation or
relevant spectral interferences from other atmospheric constituents. Modifications to the previous procedure (Mohn et al., 2010) are mainly related to the desorption phase, where the N$_2$O concentration profile was further optimized by increasing the trap tem-
perature to 10° C and decreasing the flow rate of high purity synthetic air to 10 sccm (standard cubic centimetre per minute).

### 2.2.2 Laser spectrometer

The employed QCLAS is based on the instrument described by Wächter et al. (2008). It consists of a single-mode, pulsed QCL emitting at 2188 cm$^{-1}$, a multipass absorp-
tion cell (optical path length 56 m, volume 0.5 l; Aerodyne Research Inc., USA) and a detection system with pulse normalization. Laser control, data acquisition and simul-
taneous quantification of the three main N$_2$O isotopic species ($^{14}$N$^{14}$N$^{16}$O, $^{15}$N$^{14}$N$^{16}$O,
$^{14}$N$^{15}$N$^{16}$O) is accomplished by the TDLWintel software (Aerodyne Research Inc., USA), taking into account path length, gas temperature ($\sim$ 305 K), pressure (8 kPa) and laser line width (0.0068 cm$^{-1}$). Employing a new generation thermo-electrically cooled detector (PVI-3TE-5, Vigo System, PL), a new quasi-room temperature QCL
(Alpes Lasers SA, Switzerland) and redesigned electronics led to a considerably im-
proved performance of the laser spectrometer, compared to the results of Wächter et al. (2008).

Applying the Allan variance approach (Werle, 2011) for the site-specific relative difference of isotope ratios $\delta^{15}N^{\alpha}$ and $\delta^{15}N^{\beta}$, a short term precision of 1 ‰ Hz $^{-1/2}$ is achieved at mixing ratios of 70 ppm $N_2O$, as typically obtained by preconcentration of atmospheric $N_2O$. For six minutes spectral averaging a precision below 0.1 ‰ is obtained, the maximum precision at 30 min averaging corresponds to 0.04 ‰, for both $\delta^{15}N^{\alpha}$ and $\delta^{15}N^{\beta}$.

The laser spectrometer was operated in a batch mode, where the gas cell was first evacuated by a scroll pump (TriScroll 300, Varian), then purged for 4 min with 10 sccm of purge gas at reduced pressure (1 kPa), before the downstream on-off valve (V3 in Fig. 1) (2-way, 009-0089-900, Parker Hannifin Corp., USA) was closed. The purge gas was either synthetic air (prior to analysis of preconcentrated ambient or pressurized air) or calibration gas (prior to calibration). Subsequently, the multipass cell was filled with preconcentrated air or calibration gas to a cell pressure of 8 kPa. Finally, the multipass cell was closed by switching the 3-way valve V2 or V4 (009-0933-900, Parker Hannifin Corp., USA) before the gas sample was analysed.

## 2.3 Automation and measurement procedure

The complete experimental setup including preconcentration unit, solenoid valves (V1–V6, Parker Hannifin Corp., USA) and thermal mass flow controllers (MFCs, Redy Smart series, Vögtlin Instruments, Switzerland) was controlled and monitored by a LabVIEW program (National Instruments Corp., USA). All peripherals were connected through a 16-port serial to Ethernet connector (EL-160, Digi International Inc., USA). For ambient air monitoring, a 460 min measuring cycle was repeated which consists of the following steps (Fig. 2): (A) analysis of preconcentrated $N_2O$ from compressed air (target gas, one sample) and ambient air (three gas samples), (B) analysis of standard II (two replicates) dynamically diluted to 71 ppm $N_2O$ with synthetic air to calibrate the $\delta$ scale, (C) identical to (A), (D) analysis of standard I (88 ppm $N_2O$, two replicates) to calibrate $N_2O$ mixing ratios and determine their influence on $\delta$ values. Between gas

samples (A)–(D), standard I (71 ppm $N_2O$) was analysed as a reference point and to correct for drift effects.

## 2.4 Analysis of $N_2O$ mixing ratios and isotopomer ratios

The $N_2O$ mixing ratios of ambient air were determined based on the concentration of the main isotopic species $^{14}N^{14}N^{16}O$ and calibrated against laboratory standard I dynamically diluted to different concentration levels (see Fig. 2 step D). The preconcentration step was taken into account via the ratio of the gas volume in the multipass cell ($V_{cell}$) and the gas volume applied for $N_2O$ preconcentration ($V_{precon}$). While $V_{precon}$ can be accurately computed based on the adsorption time and flow, for $V_{cell}$ this is not possible. Therefore, the exact value for $V_{cell}$ under standard conditions was determined analysing preconcentrated $N_2O$ from a highly accurate standard ($319.91 \pm 0.12$ ppb) provided by the World Meteorological Organization (WMO) Central Calibration Laboratory (CCL) (Hall et al., 2007). $N_2O$ concentrations of the laboratory standards were quantified by QCLAS against commercial calibration gases ($90.5 \pm 0.1$ ppm $N_2O$, Messer, Switzerland) and are indicated in Table 1.

Relative differences of isotopic ratios $\delta^{15}N^{\alpha}$ and $\delta^{15}N^{\beta}$ were determined employing a set of standard gases produced in our laboratory based on gravimetric and dynamic dilution methods from pure medical $N_2O$ (Messer, Switzerland) supplemented with distinct amounts of isotopically pure (>98 %) $^{15}N^{14}N^{16}O$ and $^{14}N^{15}N^{16}O$ (Cambridge Isotope Laboratories, USA). Primary laboratory standards were analysed for $\delta^{15}N^{\alpha}$, $\delta^{15}N^{\beta}$ and $\delta^{15}N^{bulk}$ by IRMS at the Tokyo Institute of Technology (Toyoda and Yoshida, 1999). Table 1 indicates the isotopic composition of the secondary laboratory standards applied in the current project and analysed against primary standards by QCLAS. The $\delta^{15}N^{bulk}$ of pure medical $N_2O$ was additionally analysed by mass spectrometry at the IsoLab of the Max-Planck Institute for Biogeochemistry (MPI-BGC, Jena, Germany) using an EA/IRMS setup (Werner et al., 1999). $N_2O$ was introduced in between the combustion and the reduction tube of the EA using the loop (250 µl) of a manually

**Site selective real-time measurements of atmospheric $N_2O$**

J. Mohn et al.

Title Page

| Abstract | Introduction |
| Conclusions | References |
| Tables | Figures |

◄ | ►

◄ | ►

Back | Close

Full Screen / Esc

Printer-friendly Version

Interactive Discussion

operated 6-port valve. This setup enabled a direct comparison of $N_2$ produced from combustion of IAEA-N1 to $N_2$ obtained from the medical $N_2O$ by reduction in the 2nd EA reactor. Quantitative $N_2O$ conversion reaction yield was verified by the absence of any $m/z$ 44 ion current response following $N_2O$ introduction. Using a $\delta^{15}N$ value of +0.43‰ for IAEA-N1 as the scale anchor, a $\delta^{15}N^{bulk}$ value of $1.64 \pm 0.10$‰ ($n = 4$) was obtained which was different by 0.39 ‰ from the Tokyo Tech result. A similar difference of 0.3‰ was observed by Toyoda and Yoshida (1999) for $\delta^{15}N^{bulk}$ of a laboratory standard calculated from $\delta^{15}N^{\alpha}$ and $\delta^{15}N^{\beta}$ (calibration via $NH_4NO_3$ decomposition) and determined after $N_2O$ to $N_2$ reduction. Discrepancies were attributed to fractionation during incomplete $NH_4NO_3$ decomposition (Toyoda and Yoshida, 1999).

Relative differences of site - selective isotope ratios $\delta^{15}N^{\alpha}$ and $\delta^{15}N^{\beta}$ of preconcentrated $N_2O$ were corrected for dependency of the isotope ratios on the $N_2O$ mixing ratio (before preconcentration). These corrections were small, about $0.004$‰ $ppb^{-1}$ and $0.016$‰ $ppb^{-1}$ for $\delta^{15}N^{\alpha}$ and $\delta^{15}N^{\beta}$, respectively. Moreover, measurements that were significantly influenced by abrupt changes in the laser intensity were discarded. These light intensity changes affected less than 2 % of the data, and the laser driver that was identified as the source of instability was recently replaced.

To confirm the accuracy of our measurements, we analysed background air in a cylinder filled in 2006 by the Earth System Research Laboratory (Global Monitoring Division) of the National Oceanic & Atmospheric Administration (NOAA). The trace gas mixing ratios analysed by the WMO CCL are typical for natural air: $384.40 \pm 0.02$ ppm $CO_2$, $319.91 \pm 0.12$ ppb $N_2O$, $1838.5 \pm 0.4$ ppb $CH_4$, $143.9 \pm 1.0$ ppb CO. The QCLAS analysis of the $N_2O$ site-selective isotopic composition, with $\delta^{15}N^{\alpha} = 15.62 \pm 0.06$‰, $\delta^{15}N^{\beta} = -2.84 \pm 0.04$‰, $\delta^{15}N^{bulk} = 6.39 \pm 0.03$‰ and SP $= 18.45 \pm 0.08$‰ (the precision indicated is the standard error of the mean), is in perfect agreement with published data for unpolluted tropospheric $N_2O$.

## 3  Results and discussion

### 3.1  Continuous analysis of N$_2$O isotopomers in ambient air

Figure 3 presents to our knowledge the first example of real-time analysis of N$_2$O site-selective isotopic composition. Measurements were conducted for three weeks between 8th and 31st September 2010, corresponding to almost 550 air samples (408 samples of ambient air, 136 target gas samples) that were analysed in stand-alone operation. During the first two weeks of the measuring campaign (up to 22nd September), N$_2$O mixing ratios display tiny but typical diurnal variations with night-time increases up to 334.2 ppb, i.e. 10 ppb above background concentrations (Fig. 3). Even though these changes in N$_2$O mixing ratios were small in the beginning, the $\delta^{15}N^{bulk}$ values display a detectable inverse trend indicating emissions of $^{15}$N depleted nitrous oxide. Substantially higher N$_2$O mixing ratios accompanied by $\delta^{15}N^{bulk}$ changes up to 10‰ were observed after fertilizer addition (200 kg N ha$^{-1}$ NH$_4$NO$_3$, 400 kg C ha$^{-1}$ sucrose) on 22 September.

Long-term precision and repeatability including preconcentration and calibration was assessed analysing a pressurized air cylinder (target gas) at every fourth preconcentration run (open symbols Fig. 3). Figure 4 displays histogram plots of repeated measurements ($n = 136$) with average N$_2$O mixing ratios of 326.47 ± 0.36 ppb and site-specific relative isotope ratio differences of $\delta^{15}N^{\alpha} = 15.28 \pm 0.24$‰ and $\delta^{15}N^{\beta} = -2.91 \pm 0.17$‰ (the precision indicated is the standard deviation). These values are consistent with background air with minor contributions from a $^{15}$N depleted N$_2$O emission source. The achieved long-term precision for $\delta^{15}N^{\alpha}$ and $\delta^{15}N^{\beta}$ is superior to state-of-the-art IRMS (Bernard et al., 2006; Toyoda et al., 2011a,b). Additionally, precision for N$_2$O mixing ratios determined by QCLAS is comparable to gas chromatography with electron capture detection (GC-ECD), the standard technique applied in global monitoring networks (Corazza et al., 2011). Besides that, as our technique has temporal averaging

capabilities, the statistical uncertainty for repeated measurements (standard error of the mean) is considerably lower.

## 3.2 Source appointment by $N_2O$ isotopomer analysis

The isotopic signature of a source process can be estimated by the Keeling-plot approach where the variations in the isotopic composition are plotted against the inverse of concentration values. This technique was originally developed for carbon dioxide and its isotopologues and has been employed in numerous studies, recently also in combination with field-deployable instrumentation for continuous $CO_2$ isotopic analysis (McManus et al., 2010; Mohn et al., 2008; Tuzson et al., 2011). For $N_2O$, up to date all process studies on $N_2O$ isotopic species had to rely on grab sampling followed by IRMS laboratory analysis because real-time analysis was not available with the required precision. Consequently, current research is based on short-term investigations with limited temporal and spatial averaging capabilities (Ostrom et al., 2010; Toyoda et al., 2011a; Yamagishi et al., 2007).

In Fig. 5, data obtained in a 24 h time interval (e.g. from 23 September noon to 24 September noon) was analysed using the Keeling plot approach. Individual data points represent the average $N_2O$ mixing ratio and isotopic composition over 20 min of $N_2O$ sampling during preconcentration. Assuming a two source mixing with unpolluted background air, the intercept of the linear regression line corresponds to the isotopic signature of the $N_2O$ emitting processes for $\delta^{15}N_s^{bulk}$ and $SP_s$. This approach implies that the soil microbial $N_2O$ production pathways and its isotopic signatures are basically constant for one diurnal cycle. As can be observed from the low scatter in the Keeling plots (i.e. Fig. 5), this model is adequate for the studied processes and gives moderate uncertainties in the linear regression parameters (Fig. 6).

Before fertilizer addition the diurnal variability in $N_2O$ mixing ratios was small, in the range of 3.0 to 10.5 ppb, accompanied by only a slight shift to lower relative isotope ratio differences at higher $N_2O$ mixing ratios. It was, nevertheless, possible to resolve these small changes and calculate daily (24 h time intervals, noon to noon) $N_2O$ source

signatures ($\delta^{15}N_s^{bulk}$, $SP_s$). These varied between $-5 \pm 7$‰ to $-26 \pm 6$‰ for $\delta^{15}N_s^{bulk}$ and $3 \pm 13$‰ to $29 \pm 5$‰ for $SP_s$ with a temporal trend (9 to 22 September) from low to high $\delta^{15}N_s^{bulk}$ and high to low $SP_s$ values (Fig. 6). Periods with changes in $N_2O$ mixing ratios below 6.5 ppb (2%) were not considered. To estimate the net isotope effect ($\Delta\delta^{15}N_s^{bulk} = \delta^{15}N(\text{substrate}) - \delta^{15}N_s^{bulk}$) of the microbial source process, the $^{15}N$ content of the substrate for $N_2O$ production needs to be known. As the focus of the present study was on method development for ambient air monitoring and not on soil science, no supplementary soil parameters were determined. However, a $\delta^{15}N$ (substrate) of 5‰ may be assumed for the inorganic soil nitrogen pool (Makarov et al., 2010). This results in a net isotope effect ($\Delta\delta^{15}N_s^{bulk}$) between 10 and 31‰, which is characteristic for $N_2O$ produced by heterotrophic denitrification. In pure culture studies with denitrifying bacteria, Sutka et al. (2006) and Toyoda et al. (2005) reported up to 39‰ for $\Delta\delta^{15}N_s^{bulk}$ of $N_2O$, and Koba et al. (2009) assigned the range 0 to 39‰ for $N_2O$ derived from heterotrophic denitrification. In contrast, $N_2O$ produced by nitrifying bacteria leads to a significantly higher $^{15}N$ depletion with a net isotope effect ($\Delta\delta^{15}N_s^{bulk} = \delta^{15}N$ ($NH_4^+$) $- \delta^{15}N_s^{bulk}$) between 46.9‰ (Sutka et al., 2006) and 68‰ (Yoshida, 1988).

The observed co-variation of $SP_s$ and $\Delta\delta^{15}N_s^{bulk}$ (Fig. 6) for $N_2O$ emitted before fertilizer application with a slope of $1.18 \pm 0.32$ can be attributed to a partial consumption by $N_2O$ reductase activity of denitrifying bacteria (Koba et al., 2009; Yamagishi et al., 2007). Similar values between 1.0 and 1.2 for $SP_s/\Delta\delta^{15}N_s^{bulk}$ were reported by Ostrom et al. (2007) for $N_2O$ reduction by two denitrifier species. The temporal trend from high to low $SP_s$ and low to high $\Delta\delta^{15}N_s^{bulk}$ values (Fig. 6) can thus be interpreted as a decreasing share of $N_2O$ reduction vs. $N_2O$ production. The $N_2O$ vs. ($N_2O + N_2$) ratio increase correlates with a night-time air temperature decrease from 13°C to 6°C at the nearby NABEL station (data not shown), which is consistent with the temperature dependence observed in laboratory studies on soil samples (Avalakki et al., 1995; Bailey and Beauchamp, 1973).

Title Page

Abstract | Introduction

Conclusions | References

Tables | Figures

◀ | ▶

◀ | ▶

Back | Close

Full Screen / Esc

Printer-friendly Version

Interactive Discussion

After fertilizer application the isotopic source signatures are better constrained because of larger diurnal changes in $N_2O$ mixing ratios (Fig. 6). Furthermore, much less variation was observed in the isotopic source signatures with values between $-0.1 \pm 0.8\,‰$ to $-5.1 \pm 1.3\,‰$ for $SP_s$ and $41.8 \pm 0.9\,‰$ to $23.2 \pm 0.7\,‰$ for $\Delta\delta^{15}N_s^{bulk}$.

To calculate the net isotope effect ($\Delta\delta^{15}N_s^{bulk} = (\delta^{15}N(\text{substrate}) - \delta^{15}N_s^{bulk})$, the $^{15}N$ content of the fertilizer N analysed by IRMS ($\delta^{15}N(NH_4NO_3) = 1.3 \pm 0.3\,‰$) was applied. The resulting $SP_s$ and $\Delta\delta^{15}N_s^{bulk}$ values are indicative for $N_2O$ production by heterotrophic denitrification without or with only minor $N_2O$ to $N_2$ reduction (Sutka et al., 2006; Toyoda et al., 2005). The observed low $N_2O$ consumption agrees with a recent publication assuming that the $N_2O/(N_2O + N_2)$ product ratio of denitrification is positively correlated with the $NO_3^-$ availability in soils (Senbayram et al., 2011). The successive increase in $\Delta\delta^{15}N_s^{bulk}$ suggests a shift in the isotope composition of the soil nitrate pool due to fractionation during denitrification.

## 4   Conclusions

This study presents to our knowledge the first real-time analysis of $N_2O$ site-selective isotopic composition at atmospheric mixing ratios. Our approach is based on a cryogenic free instrumentation which comprises a mid-IR QCL absorption spectrometer and a fully automated $N_2O$ preconcentration unit. During three weeks of continuous field measurements nearly 550 air samples were analysed for $N_2O$ mixing ratios and site-specific isotopic composition. Long term precision for $\delta^{15}N^{\alpha}$ and $\delta^{15}N^{\beta}$ was found to be superior to state-of-the-art IRMS. Additionally, precision for $N_2O$ mixing ratios determined by QCLAS was comparable to the standard technique applied in global monitoring networks (GC-ECD).

The excellent analytical precision allowed resolving even small changes in $N_2O$ mixing ratios and isotope composition, $\delta^{15}N^{bulk}$ and SP and calculating daily (24 h time intervals, noon to noon) source signatures ($\delta^{15}N_s^{bulk}$, $SP_s$) for $N_2O$ emitted from

a grassland plot. Before fertilizer application, $\Delta\delta^{15}N_s^{bulk}$ indicates heterotrophic denitrification as the main $N_2O$ production pathway. Co-variation of $SP_s$ and $\Delta\delta^{15}N_s^{bulk}$ can be attributed to a partial consumption by $N_2O$ reductase activity of denitrifying bacteria. Heterotrophic denitrification remained the main $N_2O$ production pathway after fertilization. However, the $N_2O$ reductase activity ceased due to increased $NO_3^-$ availability. As demonstrated in this feasibility study, continuous high precision analysis of $N_2O$ isotopomers at atmospheric mixing ratios can be applied for identification of $N_2O$ source processes and open a completely new field of applications.

# References

Avalakki, U. K., Strong, W. M., and Saffigna, P. G.: Measurement of gaseous emissions from denitrification of applied $^{15}N$. 2. Effects of temperature and added straw, Aust. J. Soil Res., 33, 89–99, doi::10.1071/SR9950089, 1995.

Bailey, L. D. and Beauchamp, E. G.: Effects of temperature on $NO_3^-$ and $NO_2^-$ reduction, nitrogenous gas production, and redox potential in a saturated soil, Can. J. Soil Sci., 53, 213–218, doi:10.4141/cjss73-032, 1973.

Bernard, S., Röckmann, T., Kaiser, J., Barnola, J.-M., Fischer, H., Blunier, T., and Chappellaz, J.: Constraints on $N_2O$ budget changes since pre-industrial time from new firn air and

**Site selective real-time measurements of atmospheric $N_2O$**

J. Mohn et al.

ice core isotope measurements, Atmos. Chem. Phys., 6, 493–503, doi:10.5194/acp-6-493-2006, 2006.

Brenninkmeijer, C. A. M. and Röckmann, T.: Mass spectrometry of the intramolecular nitrogen isotope distribution of environmental nitrous oxide using fragment-ion analysis, Rapid Commun. Mass Spectrom., 13, 2028–2033, doi:10.1002/(SICI)1097-0231(19991030)13:20<2028::AID-RCM751>3.0.CO;2-J, 1999.

Coplen, T. B.: Guidelines and recommended terms for expression of stable-isotope-ratio and gas-ratio measurement results, Rapid Commun. Mass Spectrom., 25, 2538–2560, 2011.

Corazza, M., Bergamaschi, P., Vermeulen, A. T., Aalto, T., Haszpra, L., Meinhardt, F., O'Doherty, S., Thompson, R., Moncrieff, J., Popa, E., Steinbacher, M., Jordan, A., Dlugokencky, E., Brühl, C., Krol, M., and Dentener, F.: Inverse modelling of European N$_2$O emissions: assimilating observations from different networks, Atmos. Chem. Phys., 11, 2381–2398, doi:10.5194/acp-11-2381-2011, 2011.

Frame, C. H. and Casciotti, K. L.: Biogeochemical controls and isotopic signatures of nitrous oxide production by a marine ammonia-oxidizing bacterium, Biogeosciences, 7, 2695–2709, doi:10.5194/bg-7-2695-2010, 2010.

Gagliardi, G., Borri, S., Tamassia, F., Capasso, F., Gmachl, C., Sivco, D. L., Baillargeon, J. N., Hutchinson, A. L., and Cho, A. Y.: A frequency-modulated quantum-cascade laser for spectroscopy of CH$_4$ and N$_2$O isotopomers, Isot. Environ. Health Stud., 41, 313–321, doi:10.1080/10256010500384572, 2005.

Hall, B. D., Dutton, G. S., and Elkins, J. W.: The NOAA nitrous oxide standard scale for atmospheric observations, J. Geophys. Res., 112, D09305, doi:10.1029/2006jd007954, 2007.

Ishijima, K., Sugawara, S., Kawamura, K., Hashida, G., Morimoto, S., Murayama, S., Aoki, S., and Nakazawa, T.: Temporal variations of the atmospheric nitrous oxide concentration and its $\delta^{15}$N and $\delta^{18}$O for the latter half of the 20th century reconstructed from firn air analyses, J. Geophys. Res., 112, D03305, doi:10.1029/2006JD007208, 2007.

Janssen, C. and Tuzson, B.: A diode laser spectrometer for symmetry selective detection of ozone isotopomers, Appl. Phys. B, 82, 487–494, doi:10.1007/s00340-005-2044-6, 2006.

Kaiser, J., Röckmann, T., and Brenninkmeijer, C. A. M.: Complete and accurate mass spectrometric isotope analysis of tropospheric nitrous oxide, J. Geophys. Res., 108, 4476, doi:10.1029/2003JD003613, 2003.

Koba, K., Osaka, K., Tobari, Y., Toyoda, S., Ohte, N., Katsuyama, M., Suzuki, N., Itoh, M., Yamagishi, H., Kawasaki, M., Kim, S. J., Yoshida, N., and Nakajima, T.: Biogeo-

chemistry of nitrous oxide in groundwater in a forested ecosystem elucidated by nitrous oxide isotopomer measurements, Geochim. Cosmochim. Acta, 73, 3115–3133, doi:10.1016/j.gca.2009.03.022, 2009.

Makarov, M. I., Leoshkina, N. A., Ermak, A. A., and Malysheva, T. I.: Seasonal dynamics of the mineral nitrogen forms in mountain-meadow alpine soils, Eur. Soil Sci., 43, 905–913, doi:10.1134/s1064229310080077, 2010.

McManus, J. B., Nelson, D. D., and Zahniser, M. S.: Long-term continuous sampling of $^{12}CO_2$, $^{13}CO_2$ and $^{12}C^{18}O^{16}O$ in ambient air with a quantum cascade laser spectrometer, Isot. Environ. Health Stud., 46, 49–63, doi:10.1080/10256011003661326, 2010.

Miller, B. R., Weiss, R. F., Salameh, P. K., Tanhua, T., Greally, B. R., Mühle, J., and Simmonds, P. G.: Medusa: a sample preconcentration and GC/MS detector system for in situ measurements of atmospheric trace halocarbons, hydrocarbons, and sulfur compounds, Anal. Chem., 80, 1536–1545, doi:10.1021/ac702084k, 2008.

Mohn, J., Zeeman, M. J., Werner, R. A., Eugster, W., and Emmenegger, L.: Continuous field measurements of $\delta^{13}$C-CO$_2$ and trace gases by FTIR spectroscopy, Isot. Environ. Health Stud., 44, 241–251, doi:10.1080/10256010802309731, 2008.

Mohn, J., Guggenheim, C., Tuzson, B., Vollmer, M. K., Toyoda, S., Yoshida, N., and Emmenegger, L.: A liquid nitrogen-free preconcentration unit for measurements of ambient N$_2$O isotopomers by QCLAS, Atmos. Meas. Tech., 3, 609–618, doi:10.5194/amt-3-609-2010, 2010.

Montzka, S. A., Reimann, S., Engel, A., Krüger, K., O'Doherty, S., Sturges, W. T., Blake, D., Dorf, M., Fraser, P., Froidevaux, L., Jucks, K., Kreher, K., Kurylo, M. J., Mellouki, A., Miller, J., Nielsen, O.-J., Orkin, V. L., Prinn, R. G., Rhew, R., Santee, M. L., Stohl, A., and Verdonik, D.: Ozone-depleting substances (ODSs) and related chemicals, Chapter 1, in: Scientific Assessment of Ozone Depletion: 2010, Global Ozone Research and Monitoring Project, Report No. 52, edited by: Ennis, C. A., World Meteorological Organization, Geneva, 516, 2011.

Nakayama, T., Fukuda, H., Kamikawa, T., Sugita, A., Kawasaki, M., Morino, I., and Inoue, G.: Measurements of the $3\nu_3$ band of $^{14}N^{15}N^{16}O$ and $^{15}N^{14}N^{16}O$ using continuous-wave cavity ring-down spectroscopy, Appl. Phys. B, 88, 137–140, doi:10.1007/s00340-007-2653-3, 2007.

Ostrom, N. E., Pitt, A., Sutka, R., Ostrom, P. H., Grandy, A. S., Huizinga, K. M., and Robertson, G. P.: Isotopologue effects during N$_2$O reduction in soils and in pure cultures of denitrifiers, J. Geophys. Res., 112, G02005, doi:10.1029/2006JG000287, 2007.

Ostrom, N. E., Sutka, R., Ostrom, P. H., Grandy, A. S., Huizinga, K. M., Gandhi, H., von Fis-

cher, J. C., and Robertson, G. P.: Isotopologue data reveal bacterial denitrification as the primary source of $N_2O$ during a high flux event following cultivation of a native temperate grassland, Soil Biol. Biochem., 42, 499–506, doi:10.1016/j.soilbio.2009.12.003, 2010.

Park, S., Atlas, E. L., and Boering, K. A.: Measurements of $N_2O$ isotopologues in the stratosphere: Influence of transport on the apparent enrichment factors and the isotopologue fluxes to the troposphere, J. Geophys. Res., 109, D01305, doi:10.1029/2003JD003731, 2004.

Ravishankara, A. R., Daniel, J. S., and Portmann, R. W.: Nitrous oxide ($N_2O$): The dominant ozone-depleting substance emitted in the 21st century, Science, 326, 123–125, doi:10.1126/science.1176985, 2009.

Röckmann, T. and Levin, I.: High-precision determination of the changing isotopic composition of atmospheric $N_2O$ from 1990 to 2002, J. Geophys. Res., 110, D21304, doi:10.1029/2005JD006066, 2005.

Schmidt, H. L., Werner, R. A., Yoshida, N., and Well, R.: Is the isotopic composition of nitrous oxide an indicator for its origin from nitrification or denitrification? A theoretical approach from referred data and microbiological and enzyme kinetic aspects, Rapid Commun. Mass Spectrom., 18, 2036–2040, doi:10.1002/rcm.1586, 2004.

Senbayram, M., Chen, R., Budai, A., Bakken, L., and Dittert, K.: $N_2O$ emission and the $N_2O/(N_2O + N_2)$ product ratio of denitrification as controlled by available carbon substrates and nitrate concentrations, Agric. Ecosyst. Environ., 147, 4–12, doi:10.1016/j.agee.2011.06.022, 2011.

Solomon, S., Qin, D., Manning, M., Alley, R. B., Berntsen, T., Bindoff, N. L., Chen, Z., Chidthaisong, A., Gregory, J. M., Hegerl, G. C., Heimann, M., Hewitson, B., Hoskins, B. J., Joos, F., Jouzel, J., Kattsov, V., Lohmann, U., Matsuno, T., Molina, M., Nicholls, N., Overpeck, J., Raga, G., Ramaswamy, V., Ren, J., Rusticucci, M., Somerville, R., Stocker, T. F., Whetton, P., Wood, R. A., and Wratt, D.: Technical Summary, in: Climate Change 2007: The Physical Science Basis. Contribution of Working Group I to the Fourth Assessment Report of the Intergovernmental Panel on Climate Change, edited by: Solomon, S., Qin, D., Manning, M., Chen, Z., Marquis, M., Averyt, K. B., Tignor, M., and Miller, H. L., Cambridge University Press, Cambridge, UK and New York, 91, 2007.

Sutka, R. L., Ostrom, N. E., Ostrom, P. H., Breznak, J. A., Gandhi, H., Pitt, A. J., and Li, F.: Distinguishing nitrous oxide production from nitrification and denitrification on the basis of isotopomer abundances, Appl. Environ. Microbiol., 72, 638–644, doi:10.1128/AEM.72.1.638-

644.2006, 2006.

Toyoda, S. and Yoshida, N.: Determination of nitrogen isotopomers of nitrous oxide on a modi-
fied isotope ratio mass spectrometer, Anal. Chem., 71, 4711–4718, doi:10.1021/ac9904563,
1999.

Toyoda, S., Yoshida, N., Miwa, T., Matsui, Y., Yamagishi, H., Tsunogai, U., Nojiri, Y., and Tsu-
rushima, N.: Production mechanism and global budget of $N_2O$ inferred from its isotopomers
in the Western North Pacific, Geophys. Res. Lett., 29, 1037, doi:10.1029/2001GL014311,
2002.

Toyoda, S., Yoshida, N., Urabe, T., Nakayama, Y., Suzuki, T., Tsuji, K., Shibuya, K., Aoki, S.,
Nakazawa, T., Ishidoya, S., Ishijima, K., Sugawara, S., Machida, T., Hashida, G., Mori-
moto, S., and Honda, H.: Temporal and latitudinal distributions of stratospheric $N_2O$ iso-
topomers, J. Geophys. Res., 109, D08308, doi:10.1029/2003JD004316, 2004.

Toyoda, S., Mutobe, H., Yamagishi, H., Yoshida, N., and Tanji, Y.: Fractionation of
$N_2O$ isotopomers during production by denitrifier, Soil Biol. Biochem., 37, 1535–1545,
doi:10.1016/j.soilbio.2005.01.009, 2005.

Toyoda, S., Suzuki, Y., Hattori, S., Yamada, K., Fujii, A., Yoshida, N., Kouno, R., Murayama, K.,
and Shiomi, H.: Isotopomer analysis of production and consumption mechanisms of $N_2O$
and $CH_4$ in an advanced wastewater treatment system, Environ. Sci. Technol., 45, 917–922,
doi:10.1021/es102985u, 2011a.

Toyoda, S., Yano, M., Nishimura, S., Akiyama, H., Hayakawa, A., Koba, K., Sudo, S., Yagi, K.,
Makabe, A., Tobari, Y., Ogawa, N. O., Ohkouchi, N., Yamada, K., and Yoshida, N.: Character-
ization and production and consumption processes of $N_2O$ emitted from temperate agricul-
tural soils determined via isotopomer ratio analysis, Global Biogeochem. Cy., 25, GB2008,
doi:10.1029/2009GB003769, 2011b.

Tuzson, B., Henne, S., Brunner, D., Steinbacher, M., Mohn, J., Buchmann, B., and Emmeneg-
ger, L.: Continuous isotopic composition measurements of tropospheric $CO_2$ at Jungfrau-
joch (3580 m a.s.l.), Switzerland: Real-time observation of regional pollution events, Atmos.
Chem. Phys., 11, 1685–1696, doi:10.5194/acp-11-1685-2011, 2011.

Uehara, K., Yamamoto, K., Kikugawa, T., and Yoshida, N.: Isotope analysis of environmen-
tal substances by a new laser-spectroscopic method utilizing different pathlengths, Sens.
Actuators B, 74, 173–178, doi:10.1016/S0925-4005(00)00729-2, 2001.

Uehara, K., Yamamoto, K., Kikugawa, T., and Yoshida, N.: Site-selective nitrogen isotopic ratio
measurement of nitrous oxide using 2 µm diode lasers, Spectrochim. Acta A, 59, 957–962,

**Site selective
real-time
measurements of
atmospheric $N_2O$**

J. Mohn et al.

Title Page

| Abstract | Introduction |
| Conclusions | References |
| Tables | Figures |

◄◄    ►►

◄    ►

Back    Close

Full Screen / Esc

Printer-friendly Version

Interactive Discussion

doi:10.1016/S1386-1425(02)00260-3, 2003.

Wächter, H. and Sigrist, M. W.: Mid-infrared laser spectroscopic determination of isotope ratios of $N_2O$ at trace levels using wavelength modulation and balanced path length detection, Appl. Phys. B, 87, 539–546, doi:10.1007/s00340-007-2576-z, 2007.

Wächter, H., Mohn, J., Tuzson, B., Emmenegger, L., and Sigrist, M. W.: Determination of $N_2O$ isotopomers with quantum cascade laser based absorption spectroscopy, Opt. Express, 16, 9239–9244, doi:10.1364/OE.16.009239, 2008.

Well, R., Flessa, H., Xing, L., Xiaotang, J., and Römheld, V.: Isotopologue ratios of $N_2O$ emitted from microcosms with $NH_4^+$ fertilized arable soils under conditions favoring nitrification, Soil Biol. Biochem., 40, 2416–2426, doi:10.1016/j.soilbio.2008.06.003, 2008.

Well, R., and Flessa, H.: Isotopologue signatures of $N_2O$ produced by denitrification in soils, J. Geophys. Res., 114, G02020, doi:10.1029/2008JG000804, 2009.

Werle, P.: Accuracy and precision of laser spectrometers for trace gas sensing in the presence of optical fringes and atmospheric turbulence, Appl. Phys. B, 102, 313–329, doi:10.1007/s00340-010-4165-9, 2011.

Werner, R. A., Bruch, B. A., and Brand, W. A.: ConFlo III – an interface for high precision $\delta^{13}C$ and $\delta^{15}N$ analysis with an extended dynamic range, Rapid Commun. Mass Spectrom., 13, 1237–1241, doi:10.1002/(sici)1097-0231(19990715)13:13<1237::aid-rcm633>3.0.co;2-c, 1999.

Yamagishi, H., Westley, M. B., Popp, B. N., Toyoda, S., Yoshida, N., Watanabe, S., Koba, K., and Yamanaka, Y.: Role of nitrification and denitrification on the nitrous oxide cycle in the eastern tropical North Pacific and Gulf of California, J. Geophys. Res., 112, G02015, doi:10.1029/2006JG000227, 2007.

Yoshida, N.: $^{15}N$-depleted $N_2O$ as a product of nitrification, Nature, 335, 528–529, doi:10.1038/335528a0, 1988.

Yoshida, N. and Toyoda, S.: Constraining the atmospheric $N_2O$ budget from intramolecular site preference in $N_2O$ isotopomers, Nature, 405, 330–334, doi:10.1038/35012558, 2000.
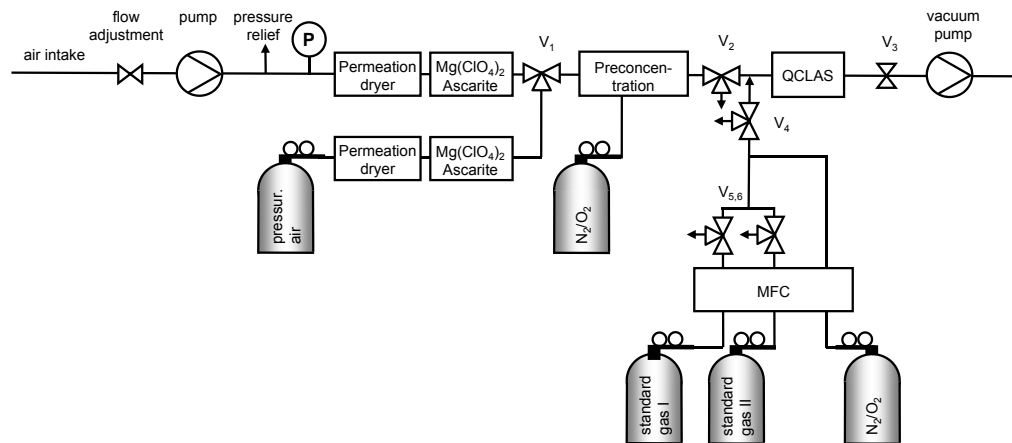
**Table 1.** N$_2$O mixing ratios and relative differences of isotopic ratios $\delta^{15}N^\alpha$ and $\delta^{15}N^\beta$ of secondary laboratory standards applied in the current project (the precision indicated is the standard error of the mean). Standard Ia was replaced by standard Ib 22 September.

|  | N$_2$O [ppm] | $\delta^{15}N^\alpha$ [‰] | $\delta^{15}N^\beta$ [‰] |
|---|---|---|---|
| Standard Ia | $246.9 \pm 0.1$ | $2.1 \pm 0.1$ | $2.0 \pm 0.2$ |
| Standard Ib | $250.1 \pm 0.05$ | $15.2 \pm 0.1$ | $2.0 \pm 0.1$ |
| Standard II | $249.1 \pm 0.1$ | $25.0 \pm 0.1$ | $24.8 \pm 0.2$ |

air intake

flow adjustment

pump

pressure relief

P

Permeation dryer

Mg(ClO$_4$)$_2$ Ascarite

V$_1$

Preconcen-tration

V$_2$

QCLAS

V$_3$

vacuum pump

Permeation dryer

Mg(ClO$_4$)$_2$ Ascarite

pressur. air

N$_2$/O$_2$

V$_4$

V$_{5,6}$

MFC

standard gas I

standard gas II

N$_2$/O$_2$

**Fig. 1.** Experimental setup for on-line N$_2$O isotopomer analysis in ambient air. Vi are solenoid valves and MFC mass flow controllers.
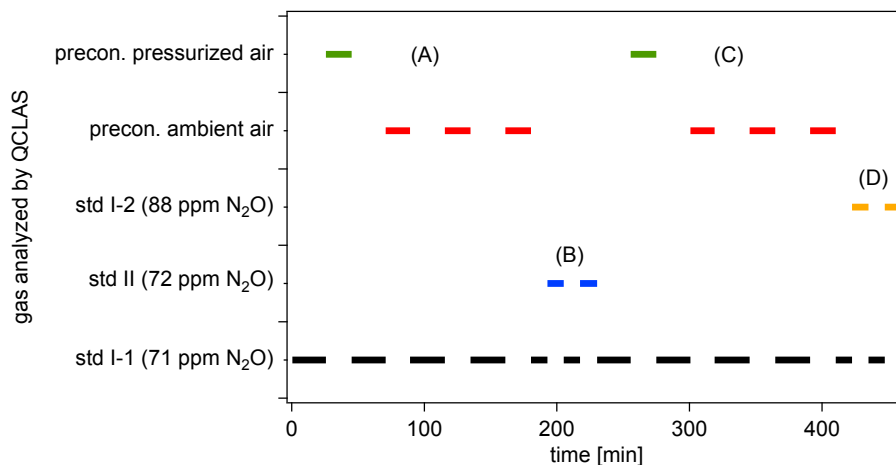
**Fig. 2.** Measurement cycle: **(A)** + **(C)** analysis of ambient air or pressurized air (target gas), **(B)** determination of calibration factors for $\delta^{15}N^{\alpha}$, $\delta^{15}N^{\beta}$, and **(D)** the N$_2$O mixing ratio as well as its influence on $\delta$ values.
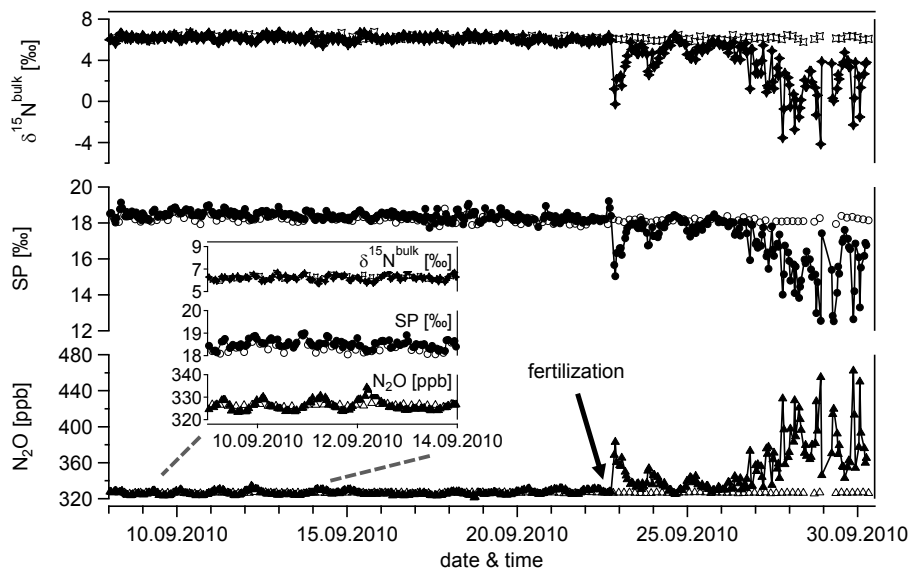
**Fig. 3.** Time series of N$_2$O mixing ratio and the corresponding $\delta^{15}$N$^{bulk}$ and SP values of ambient air (closed symbols) and pressurized air (target gas, open symbols) analysed by QCLAS after preconcentration. Relative isotope ratio differences are based on the Tokyo Tech calibration of the primary laboratory standards. Strong emissions of $^{15}$N depleted N$_2$O were observed after fertilizer addition (200 kg N ha$^{-1}$ NH$_4$NO$_3$, 400 kg C ha$^{-1}$ sucrose) indicated by an arrow.
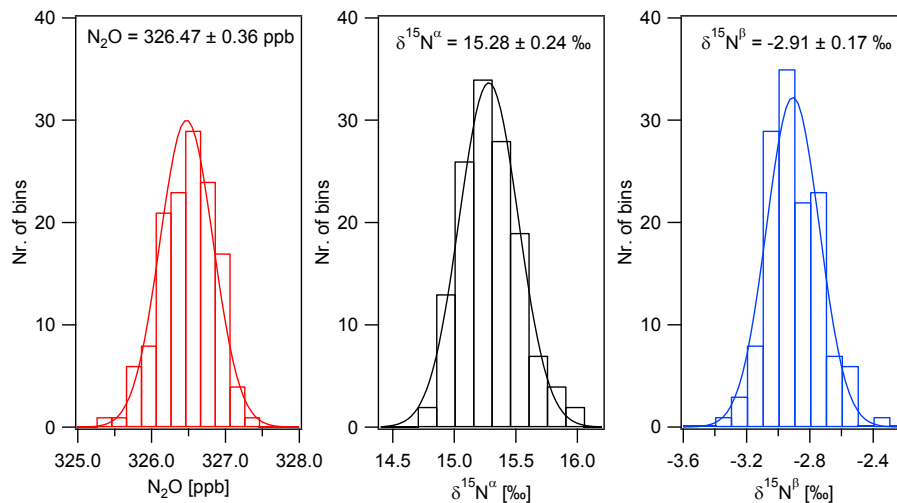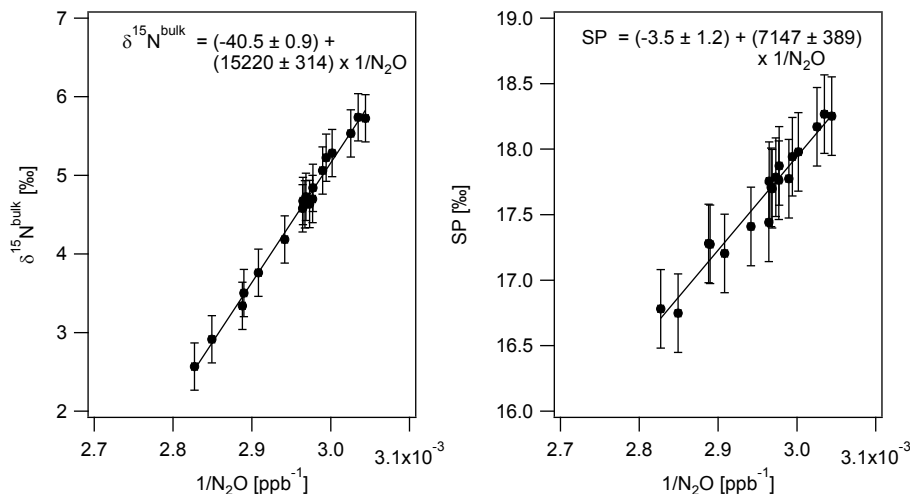
**Fig. 4.** Repeated measurements of pressurized air (target gas) during the field experiment. N$_2$O mixing ratios and relative differences of isotope ratios were plotted as a histogram with bin widths of 0.25 ppb (N$_2$O), 0.15 ‰ ($\delta^{15}N^\alpha$) and 0.1 ‰ ($\delta^{15}N^\beta$), respectively (the precision indicated is the standard deviation).

**Fig. 5.** Exemplary 24 h Keeling plot (23 September noon–24 September 2010 noon) after fertilizer addition. Site preference and $\delta^{15}N^{bulk}$ are plotted vs. the inverse of the N$_2$O concentration. The intercept of the ordinary least square linear regression corresponds to the isotopic signature of the main N$_2$O emitting process ($\delta^{15}N_s^{bulk}$, SP$_s$) and is given together with its 1$\sigma$ uncertainty.
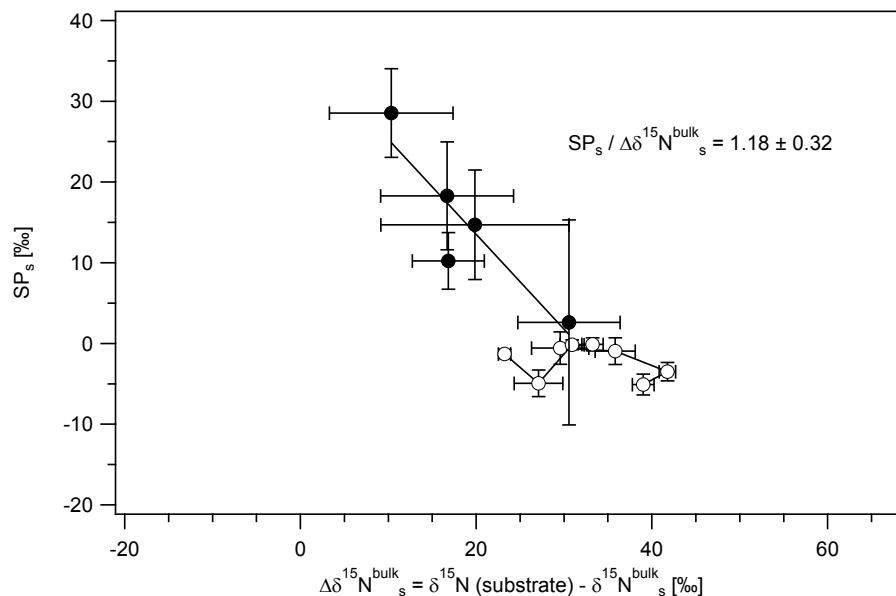
**Fig. 6.** $SP_s$ vs. $\Delta\delta^{15}N_s^{bulk}$ plot to interpret the biogeochemistry of soil emitted $N_2O$. Isotopic source signatures indicate heterotrophic denitrification as the main $N_2O$ production process, with $\Delta\delta^{15}N_s^{bulk}$ values between 10 and 42‰. Before fertilizer application (closed symbols, 9 to 22 September, periods with $N_2O$ concentration changes >6.5 ppb) a $SP_s/\Delta\delta^{15}N_s^{bulk}$ ratio of $1.18 \pm 0.32$ indicates $N_2O$ reductase activity which ceased after fertilizer addition (open symbols, 22 to 30 September) identified by low $SP_s$ values between 0 and −5‰. For $\delta^{15}N$ (substrate) 5‰ were assumed before fertilizer addition (before 22 September) according to Makarov et al. (2010), afterwards the $^{15}N$ content of the applied $NH_4NO_3$ fertilizer ($1.3 \pm 0.3$‰) was used.

Title Page

Abstract | Introduction

Conclusions | References

Tables | Figures

◄◄ | ►►

◄ | ►

Back | Close

Full Screen / Esc

Printer-friendly Version

Interactive Discussion